Properties of Carboxylated Nitrile Rubber/ Hydrotalcite Composites Containing Imidazolium Ionic Liquids

Anna Marzec,[1] *Anna Laskowska*,*[1] *Gisele Boiteux*,[2] *Marian Zaborski*,[1] *Olivier Gain*,[2] *Anatoli Serghei*[2]

Summary: In the present study, two types imidazolium salts containing the common cation 1-butyl-3-methylimidazolium-hydrophilic tetrachloroaluminate (BMIM $AlCl_4$) and hydrophobic bis(trifluoromethylsulfonyl)imide (BMIM TFSI) are analyzed for effects on the ionic conductivity and the state of cure of carboxylated nitrile rubber/ hydrotalcite composites (XNBR/HT). Imidazolium salt containing tetrachloroaluminate ions effectively participates in the crosslinking process of carboxylated nitrile rubber and contributes to an increase in the crosslink density of the composites. Hydrophobic 1-butyl-3-methylimidazolium bis(trifluoromethylsulfonyl)imide was found to be compatible with carboxylated nitrile rubber. In the presence of 15 parts per hundred rubber (phr) of BMIM TFSI, the ionic conductivity of the composites increases from 10^{-10} to 10^{-7} $S \cdot cm^{-1}$, and the glass transition temperature (T_g) of the XNBR shifts towards lower temperatures from -23 °C to -33 °C.

Keywords: carboxylated nitrile rubber; composites; crosslinking; dielectric properties; elastomers; ionic liquids

Introduction

Ionic liquids (ILs) are usually composed of organic ions and melt at or below 100 °C. Ideally, ILs are non-flammable, optically clear, have negligible volatility and high chemical stability and are relatively undemanding and inexpensive to manufacture.[1] Potential applications of ILs include the use as an alternative for traditional volatile organic solvents,[2] for catalytic reactions,[3] use in solvation of radioactive material,[4] use as antistatic additives for polymer systems and for electrochemical applications such as solar cells and actuators.[5,6] Additionally, ionic liquids can be used as viscosity adjustable agents (plasticizers), and as compatibilizers for multi-component blends which include components such as dyes, molecular fingerprint (fluorescent) agents, and antimicrobial agents. Recently, the application of ILs as a fillers dispersants for rubber matrices was shown to be a promising strategy for controlling the structure and the mechanical, thermal and dielectric properties of polymer composites. Due to their high thermal stability, ILs can easily endure the high temperatures used during the melt-blending processes and vulcanization of rubbers. While different types of fillers (carbon-nanotubes, halloysite, carbon black, silica, and layered double hydroxides) disperse better by increasing the IL amount, excess IL can act as a plasticizer and affect the mechanical properties of the resulting composites.[7,8] In numerous papers, the conductivity of carbon-nanotubes (CNTs)/rubber composites has been enhanced by using imidazolium-type ionic liquids (ILs) as dispersion agents.

[1] Institute of Polymer and Dye Technology, Technical university of Lodz, Stefanowskiego 12/16. 90924 Lodz, Poland
Fax: (+48) 426 362543;
E-mail: anna.laskowska@hotmail.com
[2] Ingénierie des Matériaux Polymères, Université Claude Bernard Lyon1, UMR CNRS 5223, 15 Bd A., Latarjet, 69622 Villeurbanne, France

For example, the presence of ionic liquids leads to a significant increase in the conductivity of CNTs/polychloroprene rubber composites.[8,9,10,11] In later work on IL-CNTs/CR composites, Subramaniam et al. reported that combining CR with ionic liquid modified CNTs causes an enhancement in thermal stability, which can be attributed to the fine dispersion of the modified tubes in the CR matrix.[12] In other investigations, the electrical conductivity of IL-CNTs/CR composites increased upon accelerated thermal aging, and therefore, the authors concluded that these composites may be useful for applications where conductivity at elevated temperatures is required.[13] The use of ILs as dispersion agents has been reported not only for CNTs in a polar polychloroprene elastomer, but also in other combinations, including: IL-CNTs-OH/hydrogenated nitrile rubber (HNBR),[14] IL-carbon black/solution-styrene-butadiene rubber (SSBR),[15] IL-CNTs/SSBR,[16] IL-CNTs/SSBR/butadiene rubber (BR),[17] silica/styrene-butadiene rubber (SBR),[18] silica/SBR,[19] halloysite nanotubes (HNTs)/SBR,[20] IL-HNTs/SBR,[21] silica/nitrile rubber NBR,[22] and layered double hydroxide (LDH)/carboxylated nitrile rubber (XNBR).[22] For applications in electrochemical devices, where flexibility, thermal stability and high ionic conductivity are required, polymer electrolytes are frequently based on NBR mixed with an ionic liquid and show greatly enhanced ionic conductivity.[23,24,25] Homogeneous distribution of fillers and increased ionic conductivity are two major reasons for the incorporation of ionic liquids in elastomer composites. However, there are some reports that claim that certain types of ILs may influence the rate of the rubber crosslinking process, and depending on the IL's composition, may reduce or extend the overall time of vulcanization.[26] For example, a series of ILs was applied to NBR to study the effect of the anions on zinc oxide nanoparticles activity in sulfur vulcanization. The authors concluded that alkylimidazolium and alkylammonium salts catalyze the interface crosslinking reactions, and consequently, the vulcanization time of the rubber compounds remarkably decreases and the crosslink density of the vulcanizates increases.[27] Incorporation of ionic liquids can help accelerate the curing process of rubbers, and may also increase the ionic conductivity and improve the state of filler dispersion of elastomer composites. Therefore, this study mainly focuses on investigation the influence of IL structure (and concentration) on the aforementioned properties of rubber composites. In this work, we studied the effects of an increasing concentration of 2.5 phr to 15 phr (parts per hundred rubber) of two types of imidazolium ionic liquids on carboxylated nitrile butadiene rubber (XNBR) composites containing magnesium aluminum layered double hydroxide (HT), where the HT acts as both a filler and a curative. The two investigated ILs have different impact on key properties of XNBR/HT, including curing kinetics, ionic conductivity, mechanical thermal and morphological properties. The first IL investigated was hydrophobic 1-butyl-3-methylimidazolium bis(trifluoromethylsulfonyl)imide, designated here as BMIM TFSI, which is a commonly applied IL in elastomer composites. The second IL investigated was hydrophilic 1-butyl-3-methylimidazolium tetrachloroaluminate, which will be further referred as BMIM $AlCl_4$.

Experimental Part

Materials

The carboxylated acrylonitrile-butadiene rubber XNBR used in this study was Krynac X 750 (7 wt% carboxyl groups content, 27 wt% acrylonitrile content, Mooney viscosity (ML1 + 4(100 °C):47)) supplied by LANXESS (Germany). Hydrotalcite, also known as magnesium aluminum layered double hydroxide MgAl-LDH, designated here as HT (Sigma Aldrich, Germany), fulfilled a filler and a curing agent function in XNBR compounds. Both of ionic liquids 1-butyl-3-methylimidazolium tetrachloroaluminate (BMIM $AlCl_4$)

and 1-butyl-3-methylimidazolium bis(trifluoromethylsulfonyl)imide (BMIM TFSI) were supplied by Sigma Aldrich (Germany).

Preparation of Composites

The HT in an amount of 30 parts per hundred rubber (phr) was mixed with different contents (2.5, 5, 10 and 15 phr) of BMIM $AlCl_4$ and BMIM TFSI by grinding it till a homogeneous paste was obtained. The rubber compounds were processed in an internal mixer Brabender Measuring Mixer N50 at 40 rpm rotors speed and the initial temperature was set at 60 °C. After around 5 minutes of rubber mastication, the mix composed of HT filler and IL was added and homogenized for around 10 minutes. Subsequently the compounded rubbers were milled in a laboratory two-roll mill (friction ratio 1:1,2, roll temperature = 40 °C, dimensions: diameter = 200 mm, length = 450 mm). The curing characteristics of XNBR/IL-HT composites were determined with a moving die rheometer (MDR 3000, MonTech, Germany) at 160 °C for 120 minutes. A sinusoidal strain of 7% and frequency of 1.67 Hz was applied. The optimum cure time (t_{90}), scorch time (t_2), minimum torque (S_{min}), maximum torque (S_{max}), and delta torque (ΔS) were determined from the curing curves. The mixed stocks were cured in a standard hot press at 160 °C, at t_{90} for the respective samples. The rubber sheets obtained from this procedure had a thickness less than 1 mm.

Testing and Characterization

The crosslink density in the vulcanized network was determined by the method of equilibrium swelling. The vulcanizates were subjected to equilibrium swelling in toluene for 48 h at room temperature. The swollen samples were then weighted on a torsion balance, dried in a dryer at a temperature of 60 °C to a constant weight and reweighed after 48 h. The crosslinking density was determined on the basis of the Flory-Rehner's equation.[28]

$$v_T = -\frac{\ln(1-V_p) + V_p + \chi \cdot V_p^2}{V_S\left(V_p^{\frac{1}{3}} - \frac{V_p}{2}\right)} \quad (1)$$

Where V_p is the volume fraction of the polymer in the swollen gel, V_S the molar volume of the solvent, and χ the Flory-Huggins interaction parameter. The Flory-Huggins interaction parameter was calculated with the Equation 2 in accordance to literature.[29,30]

$$\chi = 0.487 + 0.228 \cdot V_p \quad (2)$$

Stress-strain tests were performed with a universal material testing machine (Zwick model 1435) with a crosshead speed of 500 mm · min^{-1} according to the standard PN-ISO 37-2005. To measure mechanical properties, five different dumbbell-shaped specimens were punched from each rubber sample. The tensile strength, modulus at 100%, 200% and 300% elongation and elongation at break were measured at room temperature. DSC (differential scanning calorimetry) measurements (Q 200 DSC, TA Instrument, USA) of samples were performed at a heating rate of 10 °C · min^{-1} in the temperature range - 80 to 180 °C under a nitrogen atmosphere. The glass transition temperatures (Tg) were determined at the midpoint of the step. Dielectric measurements were conducted with broadband dielectric spectroscopy (BDS) (Novocontrol alpha analyser, Hundsagen, Germany) in the frequency range from 10^{-1} to 10^7 Hz at room temperature. The samples were placed between two copper electrodes with diameters of 20 mm. Dynamical mechanical analysis (DMA) of composites was performed with a dynamic mechanical analyzer (Q 800 DMA, TA Instrument, USA). Storage modulus (E'), loss modulus (E") and loss tangent (tan δ) were measured in tension mode in the temperature range -90 to 100 °C at a frequency of 10 Hz and a heating rate of 2 °C·min^{-1}. Thermogravimetric analysis (Q 500 TGA, TA Instruments, USA) was performed in the temperature range 50 °C to 600 °C under helium atmosphere and at a heating rate of 10 °C·min^{-1}. The fractured surfaces of the prepared materials were inspected using a scanning electron microscopy with a microscope SEM HITACHI S800 at the accelerating voltage of 15 kV. Prior to SEM-EDS observations,

liquid nitrogen-fractured surfaces of the composites were Au/Pd sputtered (with a thickness of approximately 10 nm).

Results and Discussion

Effect of ILs on the Cure Characteristics and Crosslink Density

The influence of ionic liquid type and concentration on the crosslinking process was assessed using rheometer measurements. The cure characteristics of the XNBR compounds and crosslink densities of the composites are shown in Table 1.

Applying the tetrachloroaluminate ($AlCl_4^-$) ionic liquid significantly accelerated the curing process of the XNBR/HT compound, which is reflected in an almost three-times higher cure rate index (CRI) parameter. The increased loading of BMIM $AlCl_4$ considerably shortened the scorch time (t_2) and the curing time (t_{90}) from 77 min (0 phr) to 28 min (15 phr). The incorporation of the hydrophobic TFSI salt in the rubber matrix had no significant effect on the curing kinetic of the XNBR/HT. From the rheometric data, we can observe changes in the minimum torque (S_{min}) and the maximum torque (S_{max}) during the crosslinking process. The viscosity of the rubber mix, which is reflected by changes in S_{min}, is significantly increased by the presence of $AlCl_4^-$ due to the crosslinking reaction that occurs during the processing of the rubber compound at elevated temperatures. The S_{max} increases by 300% for the system with 15 phr of BMIM $AlCl_4$, as compared to that without imidazolium salt, indicating improvement in the crosslink density. The difference between S_{max} and S_{min}, called the torque increment (ΔS), is a good indicator of the network formation. According to the data in Table 1, when the concentration of $AlCl_4^-$ increases, the ΔS significantly increases from 5.2 (control sample) to 14.8 dNm (sample with 15 phr of tetrachloroaluminate). Inversely, the increment in torque was slightly lowered by increasing the loading of $TFSI^-$, compared to the control sample of XNBR/HT. A possible reason for this is that the BMIM TFSI was acting like a plasticizer, and therefore lowered the torque parameters. The values of network densities (ν_T) of the XNBR compounds are shown in Table 1. The XNBR/BMIM $AlCl_4$-HT composites exhibited higher crosslink densities than those with $TFSI^-$ ions and the increment in ν_T was also proportional to the concentration of the tetrachloroaluminate IL. The value of ν_T increased with increasing amounts of BMIM $AlCl_4$ from 0.082 (0 phr) even up to 0.160 mmol·cm^{-3} at 15 phr loading of tetrachloroaluminate. This result is due to the curing effect of this kind of alkylimidazolium salt in the XNBR compound.

Table 1.
Rheometric characteristics and crosslink density of XNBR/IL-HT composites.

IL type and content phr	S_{min} [a] dNm	S_{max} [b] dNm	ΔS [c] dNm	t_2 [d] min	t_{90} [e] min	CRI min^{-1}	Crosslink density ν_T mmol • cm^{-3}
–	1.4	6.6	5.2	4.1	77	1.37	0.082
BMIM $AlCl_4$ 2.5	2.1	9.6	7.5	1.2	30	3.47	0.098
BMIM $AlCl_4$ 5	3.8	13.7	9.9	0.9	33	3.12	0.128
BMIM $AlCl_4$ 10	4.6	17.0	12.4	0.7	32	3.38	0.133
BMIM $AlCl_4$ 15	4.8	19.6	14.8	0.5	28	3.64	0.160
BMIM TFSI 2.5	1.2	5.4	4.2	2.6	65	1.60	0.082
BMIM TFSI 5	1.1	5.3	4.2	2.5	63	1.65	0.076
BMIM TSFI 10	1.1	4.8	3.7	3.2	64	1.64	0.069
BMIM TSFI 15	0.8	4.0	3.2	3.8	63	1.69	0.065

[a] Min. torque.
[b] Max. torque.
[c] Difference between maximum torque and minimal torque, torque increment.
[d] Scorch time.
[e] Optimal curing time.

The increasing content of BMIM TFSI leads to a decrease in the network density. The number of crosslinks (ν_T) formed in the XNBR/BMIM TFSI-HT composite decreased slightly with increasing IL concentration, indicating that the BMIM TFSI adsorbed onto the filler surface and hindered interactions between the XNBR and the magnesium aluminum layered double hydroxide HT.

Effect of ILs on Mechanical Properties

The mechanical properties of the XNBR/IL-HT composites are summarized in Table 2. While different types of fillers disperse better by increasing the IL amount, excess IL can act as plasticizer and affect the mechanical properties of the resulting composites. The highest tensile strength of the XNBR compounds with $AlCl_4^-$ ions was obtained when the IL was added at 2.5 phr and the further addition of the IL contributed to a high modulus at a relative elongation of 300% (SE_{300}), a low elongation at break (EB) and as a consequence, low tensile strength (TS). This is due to the high crosslink density. The increase in the modulus at 300% deformation (SE_{300}) correlates well with reported increment in the torque (ΔS) and the crosslink density (ν_T). The samples with increasing amounts of tetrachloroaluminate imidazolium salt exhibited lower tensile strength (TS) and elongation at break (EB) but higher hardness than those with BMIM TFSI. This can be explained through reduced mobility of the backbone chains (flexibility) and the higher number of crosslinks in the XNBR/BMIM $AlCl_4$-HT composites.

On the contrary, the opposite trends in mechanical behavior were found in the XNBR/HT composites containing $TFSI^-$ ions. In this case, the tensile strength (TS) remained almost unchanged and the elongation at break (EB) is increased slightly by increasing the IL concentration from 2.5 phr up to 10 phr. An improvement in the TS value was achieved for the composite containing 2.5 phr of BMIM TFSI, however the high concentration of imidazolium salt led to a reduced strain at break and hardness of the composites. This finding agrees with previous results, where it was shown that BMIM TFSI imidazolium salts do not increase the network density of XNBR/HT composites, but rather act as a plasticizing agent in such systems.

Effect of ILs on the Glass Transition Temperature (T_g) and Dynamic Mechanical Properties

The glass transition temperatures were measured by DSC and DMA techniques and are reported in Table 3. DSC results showed a single glass transition temperature (T_g) for all the composites, suggesting no microscopic phase separation occurred.

Table 2.
Mechanical properties of XNBR/IL-HT composites.

IL type and content phr	SE_{100}[a] MPa	SE_{200}[b] MPa	SE_{300}[c] MPa	TS[d] MPa	EB[e] %	Hardness Shore A °Sh
–	3.0 ± 0.1	5.3 ± 0.1	6.3 ± 0.1	17.6 ± 2.0	634 ± 20	62
BMIM $AlCl_4$ 2.5	3.2 ± 0.1	5.2 ± 0.2	6.9 ± 0.2	17.3 ± 2.0	600 ± 10	67
BMIM $AlCl_4$ 5	4.0 ± 0.1	6.3 ± 0.2	8.4 ± 0.3	13.5 ± 0.5	468 ± 10	70
BMIM $AlCl_4$ 10	4.2 ± 0.1	6.5 ± 0.1	8.8 ± 0.2	10.4 ± 0.4	382 ± 10	71
BMIM $AlCl_4$ 15	4.3 ± 1.0	7.1 ± 1.0	9.4 ± 1.0	9.4 ± 2.0	301 ± 10	71
BMIM TFSI 2.5	2.3 ± 0.1	4.0 ± 0.2	5.5 ± 0.2	18.2 ± 1.0	682 ± 20	62
BMIM TFSI 5	2.2 ± 0.1	3.8 ± 0.1	5.2 ± 0.1	18.0 ± 0.5	685 ± 10	62
BMIM TSFI 10	2.2 ± 0.2	3.7 ± 0.3	5.1 ± 0.5	17.5 ± 0.8	690 ± 20	62
BMIM TSFI 15	1.7 ± 0.1	2.8 ± 0.1	3.9 ± 0.1	13.4 ± 0.5	727 ± 20	59

[a] Stress modulus at 100% elongation.
[b] Stress modulus at 200% elongation.
[c] Stress modulus at 300% elongation.
[d] Tensile strength.
[e] Elongation at break.

Table 3.
Glass transition temperature (T_g) derived from DSC and DMA measurements and storage modulus (E') from dynamic mechanical measurements at 10 Hz.

IL type and content phr	T_g (DSC) °C	T_g from E" °C	T_g from tan δ °C	Height of tan δ max –	E' at 25 °C MPa
–	−23	−17.1	−6.7	1.2	10.4
BMIM $AlCl_4$ 2.5	−23	−16.9	−6.6	1.1	10.2
BMIM $AlCl_4$ 5	−24	−19.2	−6.6	1.1	10.6
BMIM $AlCl_4$ 10	−24	−19.0	−7.4	1.0	12.2
BMIM $AlCl_4$ 15	−24	−20.0	−9.7	1.0	12.7
BMIM TFSI 2.5	−24	−18.2	−8.0	1.2	11.2
BMIM TFSI 5	−26	−20.3	−9.7	1.2	9.7
BMIM TSFI 10	−28	−24.1	−12.9	1.2	9.3
BMIM TSFI 15	−33	−24.4	−14.4	1.2	9.1

The increasing amount of the $TFSI^-$ anion in the XNBR/BMIM TFSI-HT composites led to a proportional decrease of the T_g (DSC) from -23 °C (reference sample) up to -33 °C (sample with 15 phr of IL). The plasticizing effect of TFSI-containing ionic liquids on the following rubbers has been previously reported: nitrile butadiene rubber (NBR) by Marwanta,[25] hydrogenated nitrile butadiene rubber (HNBR) by Likozar[14], solution styrene butadiene rubber (SSBR)[16] and polychloroprene rubber (CR) by Subramaniam.[8,10] On the other hand, the glass transition temperature (recorded by DSC measurements) of composites containing BMIM $AlCl_4$ was unchanged at $T_g = -24$ °C regardless of the hydrophilic IL amount. These results agree with the DMA results, (Table 3), where more precise values were obtained as DMA seems to be a more sensitive technique for measuring the T_g than the DSC method.

Dynamic mechanical thermal analysis of the composites was performed at a

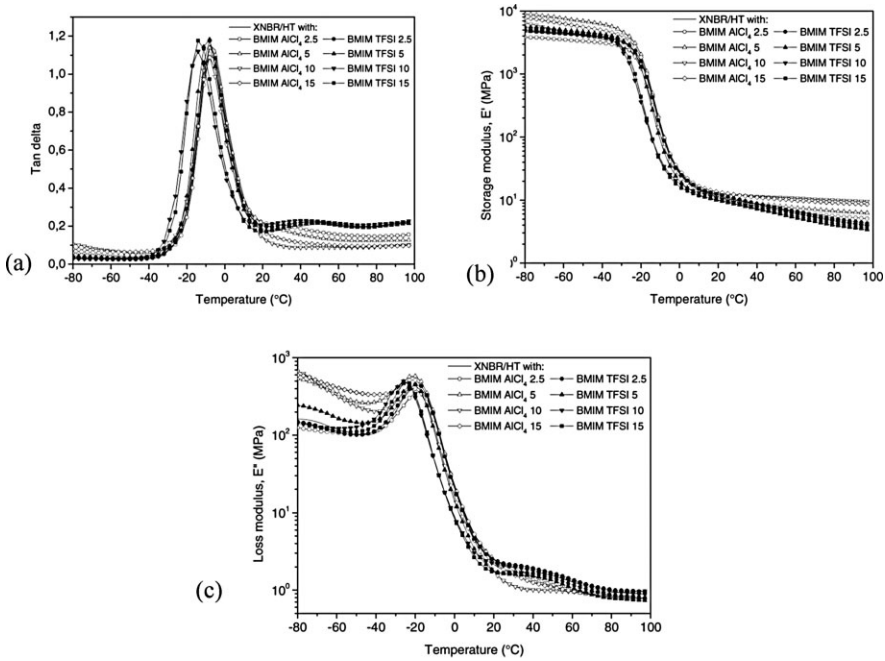

Figure 1.
(a) Plot of tan δ, (b) plot of storage modulus E' (c) plot of loss modulus E" versus temperature.

vibration frequency of 10 Hz. The value of the storage modulus (E') is reported in Table 3. Plots of the loss tangent (tan δ), storage modulus (E') and loss modulus (E") versus temperature are illustrated in Figure 1a-c. From Figure 1a, we can observe that the XNBR/HT compounds present two relaxations: one at low temperatures, which corresponds to the glass transition (T_g) of the XNBR matrix, and another from 10 °C to 50 °C with a maximum at 30 °C, corresponding to the ionic transition temperature (T_i), which indicates the existence of ionomeric clusters formed during the crosslinking of XNBR with HT.[31] These clusters melt at higher temperatures resulting in additional tan δ peaks during the DMA analysis.

What is worth to note is that the additional shoulders in the tan δ peak and in the E" plot disappeared in the presence of the hydrophilic BMIM $AlCl_4$, whereas these shoulders remained unchanged in the presence of the hydrophobic ionic liquid BMIM TFSI. The maximum of the tan δ peak of the XNBR/BMIM TFSI-HT composites shifted towards lower temperatures from -6.7 °C (control sample) up to -14.4 °C (15 phr) with increasing contents of the IL due to the plasticizing nature of BMIM TFSI in XNBR. A smaller plasticizing effect was observed for BMIM $AlCl_4$ samples containing a high concentration of tetrachloroaluminate ions, as the T_g shifted by three degrees to -9.7 °C in the presence of 15 phr of hydrophilic salt. Over the entire temperature region, the effects of BMIM $AlCl_4$ and BMIM TFSI on the storage modulus differ. Increasing the amount of BMIM $AlCl_4$ led to an enhancement in the storage modulus of the composites. The XNBR/ BMIM $AlCl_4$-HT had a remarkably higher modulus in the whole range of temperatures analyzed, whereas the presence of an ionic liquid containing $TFSI^-$ anions caused a decrease in E' in the glassy state as well as in the rubbery region.

Effect of ILs on Ionic Conductivity

As anticipated, increasing the amount of ionic liquid resulted in an increase in the ionic conductivity of the rubber composites. The improvement of AC conductivity in the XNBR/IL-HT is purely based on the contribution of ions and generally should be dependent on the conductivity and ion concentration of the pure ionic liquid. Typical values of IL conductivity measured at 25 °C range from 1.0 $mS \cdot cm^{-1}$ to 10.0 $mS \cdot cm^{-1}$. The hydrophobic BMIM TFSI has conductivity of 3.5 $mS \cdot cm^{-1}$ (25 °C) and the hydrophilic BMIM $AlCl_4$ has conductivity of 9.2 $mS \cdot cm^{-1}$ (25 °C).

The conductivity spectra of the XNBR/IL-HT composites presented in Figure 2, shows two characteristic spectral regions. At high frequencies (10^4 Hz to 10^7 Hz) an increase in the values of σ' is observed for all samples, due to local fluctuations of charge carriers giving rise to a displacement current characteristic of a capacitive regime. In the low frequencies range (0.1 Hz to 10^4 Hz), a frequency independent plateau is developed, related to long range diffusion of charge carriers giving rise to a direct current corresponding, by extrapolation, to a the DC-conductivity of the material. The transition between these two spectral regions is marked by a characteristic frequency f_e related to the hoping time of the charge carriers $\tau_e = 1/2\pi f_e$. It is observed that this characteristic frequency is shifted to higher values with increasing the concentration of the ionic liquid, which corresponds to an enhancement in the charge mobility.

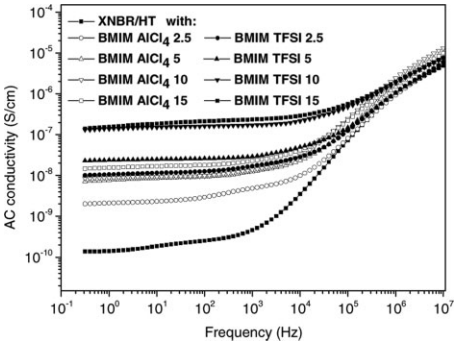

Figure 2.
AC conductivity of XNBR/IL-HT composites versus frequency, measured at room temperature.

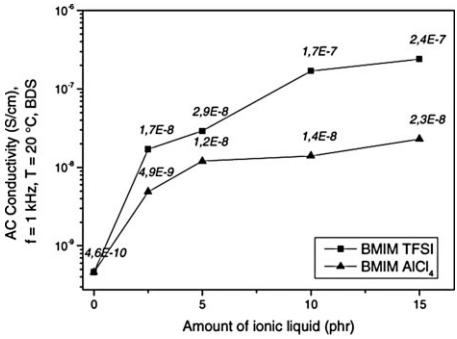

Figure 3.
AC conductivity in function of IL amount in XNBR/IL-HT composite.

The effects of the IL anion type and IL concentration on the AC ionic conductivity of XNBR/IL-HT compounds measured at 1 kHz and room temperature are illustrated in Figure 3. The incorporation of hydrophobic BMIM TFSI into XNBR/HT matrix produced composites with higher ionic conductivity in comparison to that of XNBR/BMIM $AlCl_4$-HT containing hydrophilic tetrachloroaluminate salt. The ionic conductivity increased from $4.6 \cdot 10^{-10}$ S·cm^{-1} for the control sample to $1.7 \cdot 10^{-8}$ S·cm^{-1} when 5 phr of BMIM $AlCl_4$ was added, but further increases in the hydrophilic IL amounts up to 15 phr did not alter the conductivity significantly.

Compared to BMIM $AlCl_4$, the use of hydrophobic BMIM TFSI more efficiently improves the ionic conductivity of XNBR/HT, resulting in a gradual increase to 10^{-7} S · cm^{-1} at 15 phr content of imidazolium salt. We conclude that the ionic conductivity of XNBR/IL-HT is dependent not only on the imidazolium salt concentration, but is also influenced by the plasticizing effect of the IL, which is reflected in the shift of the glass transition temperature (T_g) of XNBR towards lower temperatures. The hydrophobic BMIM TFSI contributed to the shift in the T_g from -23 °C to -33 °C whereas hydrophilic BMIM $AlCl_4$ displayed a much smaller plasticizing effect on the XNBR matrix. Significantly increased mobility of the rubber chain segment of the XNBR/BMIM TFSI-HT is surely one of the main reasons for the enhancement of ionic conductivity of the composite. Another reason for this increase is that the BMIM TFSI acts as a reservoir for effective carrier ions and raised level of these ions in the composite results in higher values of σ_{AC}. Analyzing the effects of the IL amount on the AC conductivity of a rubber material, it was found that the sharpest jump in conductivity is observed when 2.5 phr of the IL was added, and further increases in the IL content resulted in smoother changes of the σ_{AC} parameter. In summary, the ionic conductivity of XNBR/IL-HT is a function not only of the IL concentration, but is also influenced by the plasticizing effect of the IL on the rubber matrix. This effect is more pronounced in the case of hydrophobic ILs than hydrophilic ones.

Table 4.
Thermal properties of XNBR/IL-HT composites.

Anion type and content	D.T.[a] at 2% M.L.[b]	D.T. at 5% M.L.	D.T. at 10% M.L.	D.T. at 50% M.L.	M.L.[b] at 200 °C	M.L. at 600 °C	Temp. at max decomposition rate
phr	°C	°C	°C	°C	%	%	°C
–	207	291	391	445	1.8	13.45	443
$AlCl_4$2.5	198	276	383	441	2.0	14.16	442
$AlCl_4$ 5	186	287	362	440	2.3	16.25	442
$AlCl_4$ 10	144	246	336	439	3.4	16.23	436
$AlCl_4$ 15	119	187	299	436	5.5	16.36	434
TFSI 2.5	212	288	378	442	1.6	14.27	443
TFSI 5	212	284	364	441	1.6	16.81	443
TFSI 10	212	278	350	439	1.6	17.87	441
TFSI 15	212	265	340	439	1.6	22.58	438

[a] D.T. decomposition temperature.
[b] M.L. mass loss.

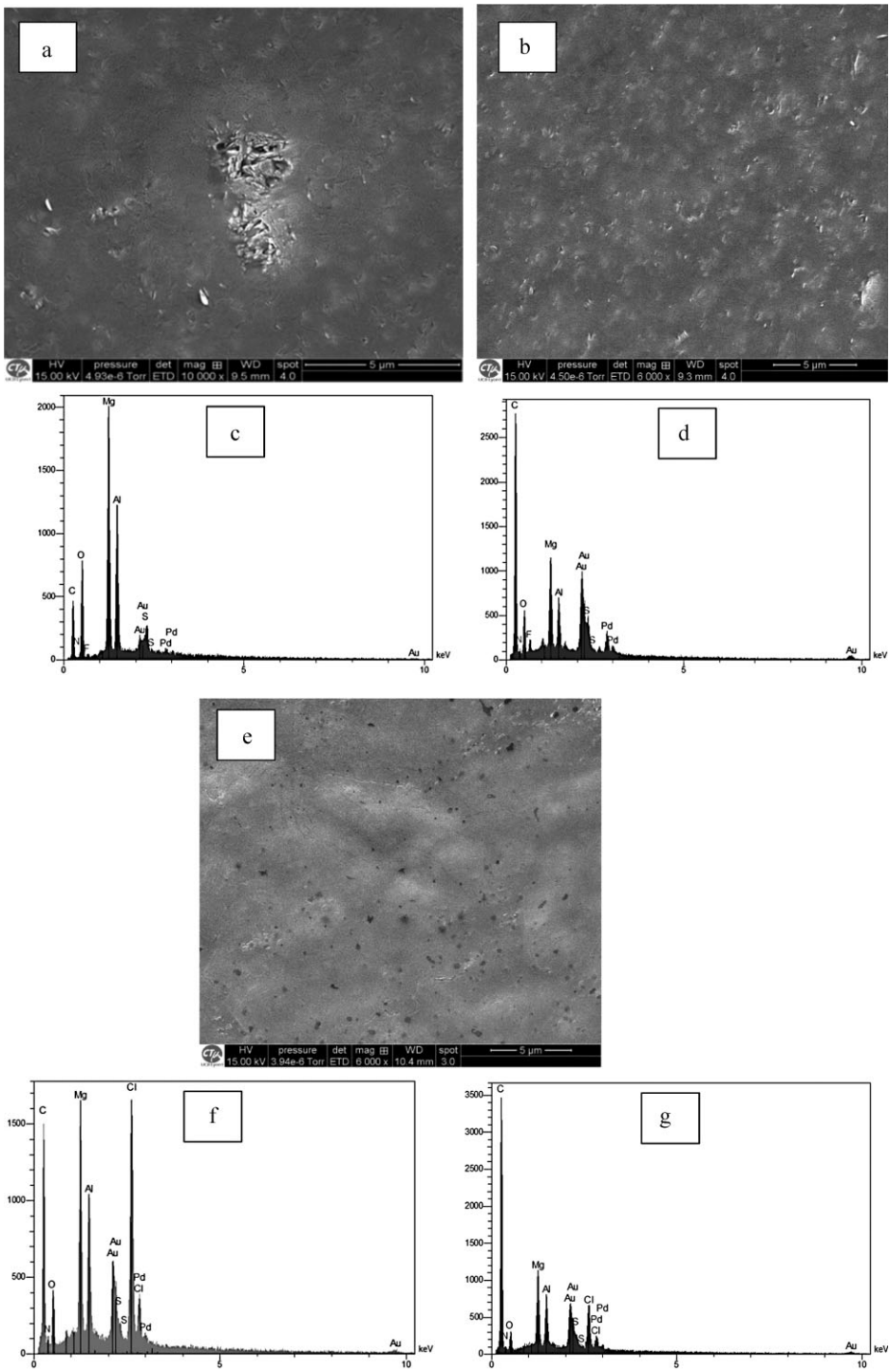

Figure 4.

SEM-EDS micrographs of (a) XNBR/HT, (b) XNBR/BMIM TFSI(5)-HT, (c) XNBR/BMIM TFSI(5)-HT filler point, (d) XNBR/BMIM TFSI(5)-HT matrix point, (e) XNBR/BMIM $AlCl_4$(5)-HT, (f) XNBR/BMIM $AlCl_4$(5)-HT filler point, (g) XNBR/BMIM $AlCl_4$(5)-HT matrix point.

Effect of ILs on Thermal Stability

The thermal properties of the XNBR/IL-HT composites characterized by a TGA/DTG technique are shown in Table 4. The TGA curves of XNBR/BMIM TFSI-HT show no thermal changes before 252.6 °C, which confirms that the BMIM TFSI ionic liquid is thermally stable in the temperature range of 25–250 °C. In the literature, it can be found that pure BMIM TFSI is thermally stable up to approximately 380 °C.[32] At higher temperatures, the TGA/DTG curves for the XNBR/BMIM TFSI-HT samples show a significant mass loss between 309 °C and 480 °C ($\Delta m = 72\%$), and a similar loss is observed in the control sample form 380 °C to 480 °C ($\Delta m = 69\%$). The TGA curves of the XNBR/BMIM $AlCl_4$-HT showed no thermal changes before 100 °C, and over 100 °C, the mass loss (M.L.) is most likely due to evaporation of water or impurities because BMIM $AlCl_4$ is a highly hygroscopic compound. The BMIM TFSI imidazolium salt exhibits superior thermal stability for elastomer processing compared to the much less thermally stable tetrachloroaluminate salt.

Effect of ILs on Morphology

The influence of ILs on the rubber composite's morphology and the distribution of HT particles in the XNBR matrix was observed by scanning electron microscopy (SEM) equipped with an energy dispersive spectrometer (EDS). The SEM-EDS micrographs of the control sample of XNBR/HT and the composites of XNBR/IL-HT containing 5 phr of IL are shown in Fig. 4(a-g). The SEM image (Figure 4a) of the XNBR/HT showed the presence of HT agglomerates greater than 5 μm in size. The composite comprised of 5 phr of the hydrophobic ionic liquid BMIM TFSI (Figure 4b) shows a better state of filler dispersion in the rubber matrix than the control sample or the sample with hydrophilic BMIM $AlCl_4$. A higher concentration of BMIM TFSI was found in the XNBR matrix (Figure 4d) than in the "filler point" (Figure 4c), what confirms good compatibility between the hydrophobic IL and the carboxylated rubber. The opposite effect was observed for the hydrophilic IL, as its concentration was found to be the highest in the "filler point" (Figure 4f) and very low in the XNBR matrix. A hydrophobic IL containing a TFSI anion is much more suitable than a hydrophilic IL with a tetrachloroaluminate anion for use as a dispersion agent. This is not only because of its higher thermal stability, but also due to its better compatibility with nitrile rubber.

Conclusion

The hydrophilic imidazolium salt BMIM $AlCl_4$ was found to be reactive toward XNBR by increasing the network density of XNBR/HT composites and significantly accelerating the curing process. The incorporation of hydrophobic TFSI ions into the XNBR/HT matrix produced composites with a higher ionic conductivity than XNBR/HT containing hydrophilic tetrachloroaluminate salt. For XNBR/HT composites, the conductivity increased about three orders of magnitude (10^{-10} to 10^{-7} $S \cdot cm^{-1}$) when 15 phr of BMIM TFSI was added. With the addition of hydrophobic BMIM TFSI, filler dispersion and ionic conductivity of the XNBR/HT composites were effectively improved. Both ionic liquids showed a plasticizing effect on the XNBR matrix, shifting the T_g towards lower temperatures with increasing concentrations of the IL, however, this effect was more pronounced in the presence of hydrophobic $TFSI^-$ ions than tetrachloroaluminate species. BMIM TFSI imidazolium salt exhibited superior thermal stability for elastomer processing compared to the much less thermally stable tetrachloroaluminate salt.

Acknowledgments: The authors wish to acknowledge the Center of Electronic Microscopy of UCB Lyon 1 (Thierry Tamet & Pierre Alcouffe) for performing electronic microscopy analysis.

[1] J. G. Huddleston, A. E. Visser, W. M. Reichert, H. D. Willauer, G. A. Broker, R. D. Rogers, *Green Chem.* **2001**, 3, 156.

[2] R. D. Rodgers, K. R. Seddon, *Science* **2003**, *302*, 792.
[3] C. M. Gordon, *Appl. Catal.* **2001**, *222*, 101.
[4] D. Allan, G. Baston, A. E. Bradley, T. Gorman, A. Haile, I. Hamblett, J. E. Hatter, M. J. F. Heasley, B. Hodgson, R. Lewin, K. V. Lovell, B. Newton, W. R. Pitner, D. W. Rooney, D. Sanders, K. R. Seddon, H. E. Sims, R. C. Thied, *Green Chem.* **2002**, *2*, 152.
[5] W. Lu, A. G. Fadeev, B. Qi, E. Smela, B. R. Mattes, J. Ding, G. M. Spinks, J. Mazurkiewicz, D. Zhou, G. C. Wallace, D. R. MacFarlane, S. A. Forsyth, M. Forsyth, *Science* **2002**, *297*, 983.
[6] J. M. Pringle, J. Golding, C. M. Forsyth, G. B. Deacon, M. Forsyth, D. R. MacFarlane, *J. Mater. Chem.* **2002**, *12*, 3475.
[7] M. Tunckol, J. Durand, P. Serp, *Carbon* **2012**, *50*, 4303.
[8] K. Subramaniam, A. Das, G. Heinrich, *Comp. Sci. Technol.* **2011**, *71*, 1441.
[9] D. Steinhauser, K. Subramaniam, A. Das, G. Heinrich, M. Kluppel, *Express Polym. Lett.* **2012**, *11*, 927.
[10] K. Subramaniam, A. Das, D. Steinhauser, M. Kluppel, G. Heinrich, *Eur. Polym. J.* **2011**, *47*, 2234.
[11] H. H. Le, X. T. Hoang, A. Das, U. Gohs, K. W. Stoeckelhuber, R. Boldt, G. Heinrich, R. Adhikari, H. J. Radush, *Carbon* **2012**, *50*, 4543.
[12] K. Subramaniam, A. Das, L. Haußler, C. Harnisch, K. W. Stockelhuber, G. Heinrich, *Polym. Degrad. Stab.* **2012**, *97*, 776.
[13] K. Subramaniam, A. Das, G. Heinrich, *Comp. Sci. Technol.* **2013**, *74*, 14.
[14] B. Likozar, *Soft Matter.* **2011**, *7*, 970.
[15] H. Kreyenschulte, S. Richter, T. Gotze, D. Fisher, D. Steinhauser, M. Kluppel, G. Heinrich, *Carbon* **2012**, *50*, 3649.
[16] K. Subramaniam, A. Das, F. Simon, G. Heinrich, *Eur. Polym J.* **2013**, *49*, 345.
[17] A. Das, K. W. Stockelhuber, R. Jurk, J. Fritzsche, M. Kuppel, G. Heinrich, *Carbon* **2009**, *47*, 3313.
[18] Y. D. Lei, Z. H. Tang, B. C. Guo, L. X. Zhu, D. M. Jia, *Express Polym. Lett.* **2010**, *11*, 692.
[19] Y. Lei, Z. Tang, L. Zhu, B. Guo, D. Jia, *J. Appl. Polym. Sci.* **2012**, *123*, 1252.
[20] Y. D. Lei, Z. H. Tang, L. X. Zhu, B. C. Guo, D. M. Jia, *Polymer* **2011**, *52*, 1337.
[21] B. Guo, X. Liu, W. Y. Zhou, Y. Lei, D. Jia, *J. Macromol. Sci. Phys.* **2010**, *49*, 1029.
[22] A. Laskowska, A. Marzec, G. Boiteux, M. Zaborski, O. Gain, A. Serghei, *Polym Int.* **2013**, *62*, 1575.
[23] E. Marwanta, T. Mizumo, H. Ohno, *Solid State Ionics* **2007**, *178*, 227.
[24] M. Cho, H. Seo, J. Nam, H. Choi, J. Koo, Y. Lee, *Sens Actuators B* **2007**, *128*, 70.
[25] E. Marwanta, T. Mizumo, N. Nakamura, H. Ohno, *Polymer* **2005**, *46*, 3795.
[26] J. Pernak, F. Walkiewicz, M. Maciejewska, M. Zaborski, *Ind. Eng. Chem. Res.* **2010**, *49*, 5012.
[27] M. Przybyszewska, M. Zaborski, *J. Appl. Polym. Sci.* **2010**, *116*, 155.
[28] P. J. Flory, J. Rehner, *J. Chem. Phys.* **1943**, *11*, 521.
[29] D. Lenko, S. Schlogl, A. Temel, R. Schaller, A. Holzner, W. Kern, J. Appl. Polym. Sci. **2013**, DOI: 10.1002/APP. 38983
[30] M. Zaborski, A. Kosmalska, J. Gulinski, *Kautsch. Gummi Kunstst.* **2005**, *58*, 354.
[31] A. Das, D. Y. Wang, K. W. Stockelhuber, R. Jurk, J. Fritzsche, M. Kuppel, G. Heinrich, *Adv. Polym. Sci.* **2011**, *239*, 85.
[32] A. A. M. Beigi, M. Abdouss, M. Yousefi, S. M. Pourmortazavi, A. Vahid, *J. Mol. Liq.* **2013**, *177*, 361.

